

Nernst effect and diamagnetism in phase fluctuating superconductors

Daniel Podolsky^{1,2}, Srinivas Raghu^{3,4}, and Ashvin Vishwanath^{1,2}

¹*Department of Physics, University of California, Berkeley, CA 94720*

²*Materials Sciences Division, Lawrence Berkeley National Laboratory, Berkeley, CA 94720*

³*Department of Physics, Princeton University, Princeton, NJ 08544*

⁴*Physics Department, Stanford University, Stanford, CA 94305*

(Dated: Printed September 18, 2018)

When a superconductor is warmed above its critical temperature T_c , long range order is destroyed by fluctuations in the order parameter. These fluctuations can be probed by measurements of conductivity[1], diamagnetism[2] and of the Nernst effect[3, 4, 5]. Here, we study a regime where superconductivity is destroyed by phase fluctuations arising from a dilute liquid of mobile vortices. We find that the Nernst effect and diamagnetic response differ significantly from Gaussian fluctuations – in particular, a much sharper decay with temperature is obtained. We predict a rapid onset of Nernst signal at a temperature T_{onset} that tracks T_c , rather than the pairing temperature. We also predict a close quantitative connection with diamagnetism – the ratio of magnetization to transverse thermoelectric conductivity α_{xy} reaches a universal value at high temperatures. We interpret Nernst effect measurements on the underdoped cuprates in terms of a dilute vortex liquid over a wide temperature range above T_c .

In recent years, the Nernst effect has emerged as an important probe of strongly-correlated electron systems. The Nernst signal is the electric field (E_y) response to a transverse temperature gradient $\nabla_x T$,

$$e_N \equiv \frac{E_y}{-\nabla_x T} \Big|_{J=0} \quad (1)$$

A large Nernst signal has been detected in the normal state of quasi-2d cuprate[3] and heavy fermion[4] samples, and in thin films[5], well above T_c . This is in contrast with typical (non-ambipolar) metals, where the Nernst effect is usually weak: it was shown[6] that Fermi liquid quasiparticles with energy-independent scattering rates do not contribute to the Nernst signal. This, together with the proximity of the large-Nernst region in some of these materials to superconducting phases, points towards fluctuating superconductivity as one natural source for the Nernst signal.

Theoretical studies of the Nernst effect in cuprate superconductors include the analysis of Gaussian fluctuations above the mean-field transition temperature[10], and a Ginsburg-Landau model with interactions between fluctuations of the order parameter[12]. In this Letter, we consider the Nernst effect due to thermal fluctuations in a phase-only model. Throughout, we assume that the superconducting order parameter $\psi(x) = \Delta_0 e^{i\theta(x)}$ has a frozen amplitude $\Delta_0(x) = \text{const}$. Such a situation can arise in granular thin films and in Josephson junction arrays, where the order parameter on individual grains is well-established, whereas T_c is given by the weak Josephson coupling between grains. This picture may also be appropriate for the underdoped cuprates, where the pairing gap is thought to be much larger than the transition temperature, $k_B T_c \ll \Delta$ [7, 8]. Here, superconductivity is destroyed by loss of phase coherence via thermally generated vortex anti-vortex pairs. Phase fluctuations from

vortex diffusion have been proposed as the dominant contribution to the Nernst signal[3, 9]. This vortex picture is most useful in the dilute limit, when the spacing between vortices (both field induced and thermally generated) is much larger than their core radius (the zero temperature coherence length ξ_0). Then, vortices have a well defined identity and the amplitude is suppressed only in the small area of the sample occupied by vortex cores.

Our starting point is the Lawrence-Doniach model of a layered superconductor,

$$\begin{aligned} F_{LD} = & -\mathcal{J} \sum_n \sum_{\langle ij \rangle} \{ \psi_{j,n}^* e^{iA_{ij}} \psi_{i,n} + \text{h.c.} \} \\ & -\mathcal{J}_\perp \sum_{\langle nm \rangle} \sum_i \{ \psi_{i,n}^* \psi_{i,m} + \text{h.c.} \} \\ & +U \sum_n \sum_i (|\psi_{i,n}|^2 + r/2U)^2 \end{aligned} \quad (2)$$

where i, j label lattice points within a layer, and n, m label the layers. The lattice vector potential due to an external magnetic field, $A_{ij} = \frac{2e}{\hbar} \int_{\mathbf{r}_i}^{\mathbf{r}_j} \mathbf{dr} \cdot \mathbf{A}$, is static and unscreened, corresponding to an extreme type-II superconductor. We consider the limit deep in the ordered phase within mean field theory $-r \gg k_B T$, where phase fluctuations dominate $\psi_{i,n} = \Delta_0 e^{i\theta_{i,n}}$. This reduces the model above to an XY model. The inter-layer coupling \mathcal{J}_\perp stabilizes true long-range superconductivity. However, we have verified that realistic values of \mathcal{J}_\perp increase T_c relative to the 2D Kosterlitz-Thouless transition T_{KT} only by a small amount, and that the normal state properties of interest are not significantly affected by \mathcal{J}_\perp , except very close to T_c . Hence, in what follows we set $\mathcal{J}_\perp = 0$ and consider the 2D XY model with Josephson coupling $J = \Delta_0^2 \mathcal{J}$.

To study transport, we supplement this statistical mechanics model with model-A Langevin dynamics, corresponding to interaction with a heat bath that does not

preserve any conservation laws[14]:

$$F_{XY} = -J \sum_{\langle ij \rangle} \cos(\theta_i - \theta_j - A_{ij})$$

$$\tau \partial_t \theta_i = -\frac{\partial F_{XY}}{\partial \theta_i} + \eta_i(t). \quad (3)$$

Here, τ provides a characteristic time scale for the dynamics. The stochastic noise $\eta_i(t)$ is Gaussian correlated, with a variance chosen to satisfy the fluctuation-dissipation theorem,

$$\langle \eta_i(t) \eta_j(t') \rangle = 2k_B T \tau \delta_{ij} \delta(t - t'). \quad (4)$$

The model (3), and (4) has only three free parameters: J , τ , and the lattice constant, a (or equivalently a field scale, $H_0 = \Phi_0 / (2\pi a^2)$, defined via the superconducting flux quantum Φ_0). Of these, J is an overall energy scale, set by fixing T_{KT} . The length scale a depends on the physical system in question. For Josephson junction arrays or granular superconductors, this is the spacing between grains. For uniform superconductors, a can be determined by comparing the correlation length in the XY model away from the transition, eg. at $T = 2T_c$, with the typical separation between thermally induced vortices at that temperature. Thus, a is given by a combination of vortex fugacity and core radius ξ_0 [20]. Within ξ_0 , the superconducting amplitude is significantly suppressed. Hence, the dilute limit, where the separation between vortices exceeds ξ_0 , determines the temperature window over which a phase-only description is appropriate. Finally, the time scale τ does not affect thermodynamic quantities, such as magnetization, nor does it enter the transverse thermoelectric conductivity, α_{xy} , which is closely related to the Nernst effect,

$$e_N = \frac{\alpha_{xy}}{\sigma_{xx}}, \quad (5)$$

where σ_{xx} is the electrical conductivity, and we have assumed particle-hole symmetry. Hence, α_{xy} and magnetization predicted by this model are only functions of T/T_{KT} and H/H_0 .

By an Onsager relation, the transverse thermoelectric conductivity α_{xy} can be obtained either from the electric current response to a temperature gradient, $j_{tr,x} = -\alpha_{xy} \nabla_y T$, or from the heat current response to an electric field, $j_{tr,x}^Q = T \alpha_{xy} E_y$. A third method to compute α_{xy} is through a Kubo formula involving the unequal time correlator $\langle j_x(t) j_y^Q(0) \rangle$. As a check of our numerics, and of the use of proper magnetization subtractions[13], we confirmed that all three methods agree for a representative set of temperatures and magnetic fields.

Intermediate Temperature Regime: The results for α_{xy}^{2d} on a single layer are shown in Figs. 1 and 2. As noted above, α_{xy} is independent of the parameter τ . For a single layer, its value only depends on the ratios T/T_{KT}

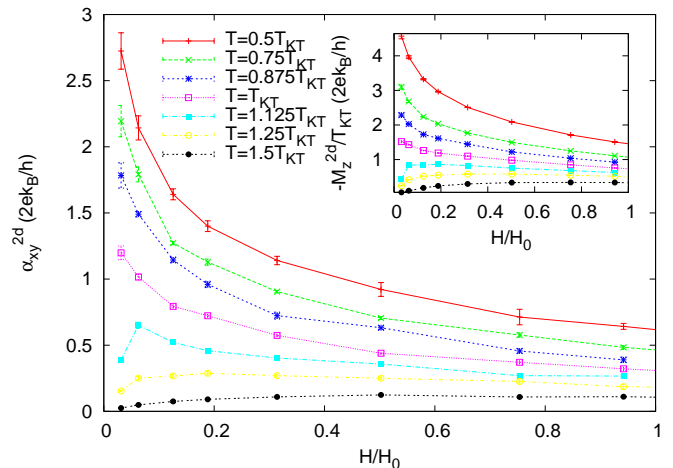


FIG. 1: Transverse thermoelectric conductivity for a single plane, in units of the quantum of thermoelectric conductance $2ek_B/h$. Simulations on a cylindrical geometry, with system size ranging from 60×60 to 200×200 . *Inset:* Diamagnetic response. Temperatures as in the main figure.

and H/H_0 , and is expressed naturally in units of the 2D “quantum of thermoelectric conductance”, $2ek_B/h$. To compare with thin film and layered systems, one must divide by the film thickness/layer separation d , $\alpha_{xy} = \alpha_{xy}^{2d}/d$. The inset of Fig. 1 shows the diamagnetic response. Below T_c , the magnetization diverges logarithmically in H . The magnetization edge currents correspond to a “depletion layer” near the edge of the sample, where vortex density is smaller than the density in the bulk, H/Φ_0 . In the vortex picture, magnetization is analogous to the work function in a metal, and we find[17], to leading order in H ,

$$M_z^{2d} = -\frac{2e}{h} \left(\frac{\pi \rho_s}{2} - k_B T \right) \log \frac{H_0}{H} \quad (6)$$

This is similar to a previous result[15], and is in good agreement with our simulations.

High Temperature Expansion: For $T \ll J$, the phase-only model allows for an analytically tractable regime that is entirely different from the Gaussian regime considered previously[10]. The high temperature expansion, carried out in powers of $J/k_B T$, is conveniently performed using the Martin-Siggia-Rose formalism[16, 17]. Since both M_z and α_{xy} require a magnetic field, the expansion of these quantities involves graphs enclosing finite a magnetic flux. The leading term thus depends on the smallest closed graph – on a square lattice this involves 4 links, and is hence proportional to $(J/T)^4$, whereas on a triangular lattice it goes as $(J/T)^3$:

$$\alpha_{xy}^{2d} = \lambda \frac{2ek_B}{h} \left(\frac{J}{T} \right)^\mu \sin \frac{H}{H_0} \quad (7)$$

$$\frac{M_z^{2d}}{T} = -2\lambda \frac{2ek_B}{h} \left(\frac{J}{T} \right)^\mu \sin \frac{H}{H_0}$$

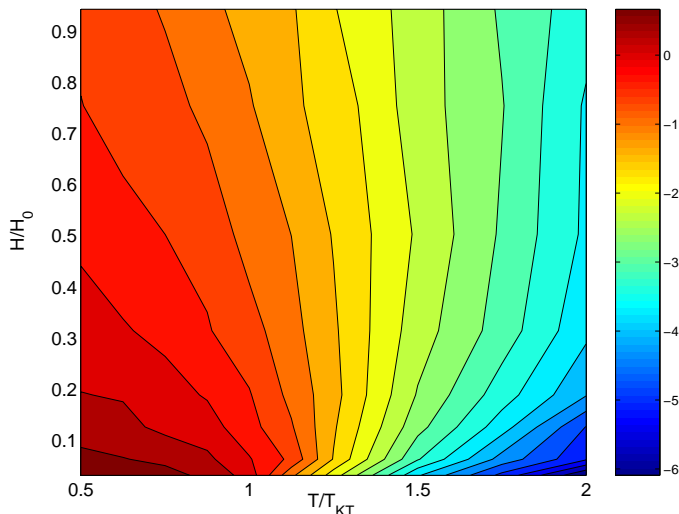


FIG. 2: Contour plot of $\log[\alpha_{xy}^{2d}/(2ek_B/h)]$. For small T and H , an inter-layer Josephson coupling J_{\perp} , absent in these simulations, stabilizes 3d superconductivity. Note that, unlike the Nernst signal $e_N = \alpha_{xy}/\sigma_{xx}$ in Ref. [3], there is no ridge field in our simulations of α_{xy} . The difference is likely due to the diverging electrical conductivity σ_{xx} as T_c is approached.

$$\frac{|M_z^{2d}|}{T\alpha_{xy}^{2d}} = 2. \quad (8)$$

Here, $\mu = 4$ and $\lambda = \pi/8$ ($\mu = 3$ and $\lambda = \pi/4$) for a square (triangular) lattice. Despite the lattice-dependent behavior of α_{xy} and M_z/T , their ratio (8) is equal to -2 , independent of the lattice. The same value of -2 is obtained in the Gaussian regime of the dynamical Ginzburg-Landau equation[10, 11], and seems to be a robust feature of fluctuating superconductivity at high temperatures. The ratio $|M_z|/T\alpha_{xy}$, shown in Fig. 3, is only weakly field-dependent, and tends to 2 at high-temperatures. This points to a close quantitative connection between the Nernst effect and diamagnetism [2].

Comparison to Nernst Measurements in the Cuprates: Experimental measurements of both Nernst voltage and conductivity are required to obtain α_{xy} . Such experimental data is available on underdoped $\text{La}_{2-x}\text{Sr}_x\text{CuO}_4$ ($x = 0.12$ and $T_c = 28$ K) in weak fields. This is shown in Fig. 4, which displays the Nernst coefficient times conductivity, $\nu\sigma_{xx} = \left. \frac{d\alpha_{xy}}{dH} \right|_{H=0}$. To compare, we choose in our simulation, $J = J_l \equiv 30.2$ K, corresponding to $T_c = 1.04T_{KT}$, and $H_0 = 50$ T (for this sample, $H_{c2} \approx 100$ T, hence $H_{c2} > H_0$, consistent with a relatively dilute vortex liquid). With these values, the simulation gives good agreement with absolute experimental values in the regime $T_c < T < 2T_c$ K, except for the very lowest temperature point $T = 30$ K. This is very close to T_c , so that 3d superconducting fluctuations, ignored here, are likely dominant.

Comparison with High Temperature Data: The inset

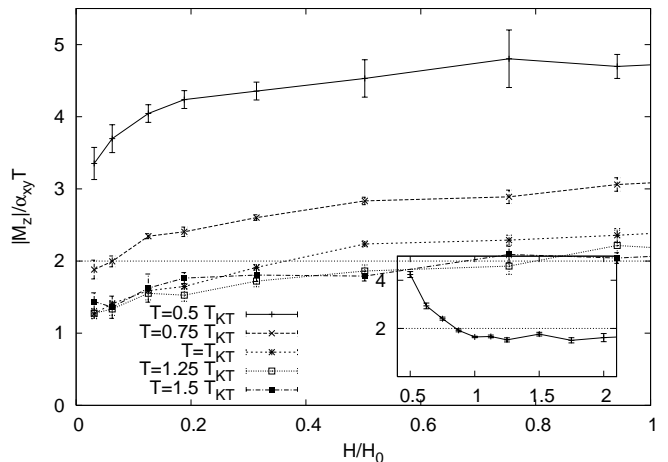


FIG. 3: The dimensionless ratio $|M_z|/T\alpha_{xy}$, as a function of magnetic field for various temperatures. In the high-temperature limit, this dimensionless ratio is expected to saturate at a value of 2 for all magnetic fields. *Inset:* $|M_z|/T\alpha_{xy}$ for $H = 0.31H_0$ vs. T/T_{KT}

of Fig. 4 shows the measured $\nu\sigma_{xx}$ on a log-log plot extending to $T = 120\text{K} \approx 4T_c$. The data displays a rapid decay over a large temperature range, in general agreement with our expectations. In particular, a T^{-4} decay is observed, which is the high temperature result (7) on a square lattice. However, since in the high temperature regime the precise power depends strongly on lattice geometry (in contrast to the intermediate temperature regime) justification for using a nearest neighbor square lattice model (as opposed to, say, a triangular lattice model) is required. While the underlying d -wave symmetry of the cuprates, coupled with the fact that a is a microscopic length, about 6 times the lattice spacing, may be invoked, whether these are sufficient to justify the square lattice model is unclear at present and requires further work.

The characteristic scale of α_{xy} at these temperatures is enhanced from what one would expect for a superconductor with $T_c = 28\text{K}$. For example, the best fit to the square lattice high temperature expansion (solid line) requires $J = J_h = 52\text{K}$, larger than the effective coupling $J_l = 30.2$ K that yields the correct T_c . This may be naturally attributed to thermal d -wave quasiparticles, omitted in this analysis, which suppress the long distance superfluid density[19] but not the superfluid density at shorter scales[17], which controls the high temperature behavior. The ratio $J_h/J_l = 1.6$ is consistent with measurements of the temperature dependent superfluid density in other cuprates [18]. A prediction from this scenario is that magnetization should continue to track $\alpha_{xy}T$.

Onset Temperature: Ong and collaborators[3] define a temperature T_{onset} where the fluctuating contribution to

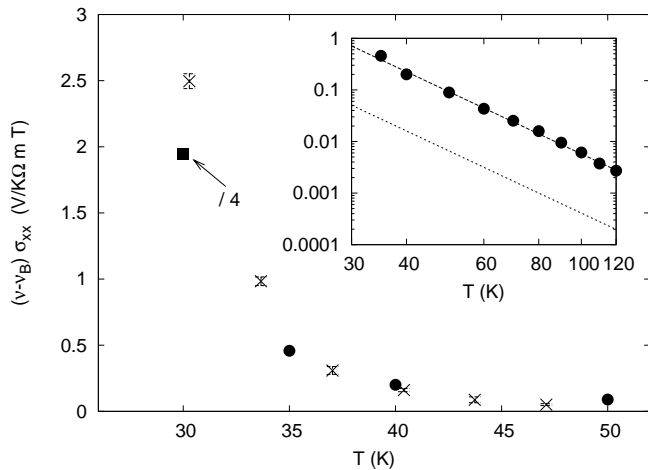


FIG. 4: Comparison to underdoped $\text{La}_{2-x}\text{Sr}_x\text{CuO}_4$ ($x = 0.12$, $T_c = 28$ K). The experimental data[3], shifted by a constant quasiparticle background contribution $\nu_B \sigma_{xx} = -0.011 \text{ V/K}\Omega \text{ m T}$, is indicated by \bullet . Simulation results are shown by X with error bars. The value of the experimental point at $T = 30 \text{ K}$ (\blacksquare) has been divided by 4 to fit in the figure. This point is very close to T_c , and hence $\nu \sigma_{xx}$ is likely dominated by 3d fluctuations, not considered in our simulations.

the Nernst effect can no longer be experimentally distinguished from the quasiparticle background. Here, since we have a natural scale for α_{xy} , we define T_{onset} as the temperature where α_{xy}^{2d} has decayed to a small fraction δ of the quantum of thermoelectric conductivity,

$$\alpha_{xy}^{2d}(T_{\text{onset}}, H) = \frac{2ek_B}{h} \delta \quad (9)$$

For our model, $\alpha_{xy}^{2d} = \frac{2ek_B}{h} F(T/T_{KT}, H/H_0)$, hence T_{onset} is proportional to T_c . The essential point is that, because α_{xy}^{2d} depends strongly on temperature, when inverted, T_{onset} is only a weak function of δ and H . For instance, the choice $H = H_0/4$ and $\delta = 0.01$ on the square lattice yields

$$T_{\text{onset}} \approx 3T_c \quad (10)$$

This is consistent with the observation that the experimentally-defined T_{onset} roughly tracks T_c as doping is varied[3]. Due to the strong temperature dependence of α_{xy} , the onset of Nernst effect is very sharp, in contrast to Gaussian fluctuations[10], where α_{xy} only decays as $1/(T_c - T)$ at high temperatures.

Experimentally, measurements of the electrical conductivity σ_{xx} do not have discernable contributions due to fluctuating superconductivity at temperatures of order T_{onset} [1]. Since σ_{xx} is proportional to the parameter τ appearing in Eq. (3), this places a constraint on the maximum value of τ . The high temperature expansion yields

$$\sigma_{xx,\text{fluct}}^{2d} = \frac{4e^2}{h} \frac{\pi J_{\text{eff}}^2 \tau}{4T^2 h}.$$

As a benchmark, we note that BCS theory predicts the value $\tau_{\text{BCS}} \approx 0.7\hbar$. This yields a fluctuating conductivity at $T = 2T_c$ that is only about 10% of the quasiparticle conductivity in this material.

In conclusion, we have studied the transverse thermoelectric conductivity α_{xy} and the diamagnetic response M^z in the classical XY model with model-A dynamics. We have obtained numerical results at low temperatures, and analytic results at high temperatures, that are functions only of two variables, T/T_c and H/H_0 , where $H_0 < H_{c2}$ is a characteristic field scale set by vortex parameters. In our model, we predict that α_{xy} and M^z for different systems (e.g. different dopings) should collapse into a single curve when expressed in terms of the system-dependent T_c and H_0 . We show that M^z/T and α_{xy} track each other and, in particular, we predict that their ratio tends to -2 at high temperatures. Measurements of α_{xy} on the underdoped cuprate $\text{La}_{1.88}\text{Sr}_{0.12}\text{CuO}_4$ display a sharp temperature decay, in agreement with our model.

We would like to thank P.W. Anderson, D. Huse, S. Kivelson, J.E. Moore, S. Mukerjee, N.P. Ong, and Y. Wang for many insightful discussions.

-
- [1] J. Corson, R. Malozzi, J. Orenstein, J. N. Eckstein, and I. Bozovic, *Nature* **398**, 221 (1999)
 - [2] Y. Wang, *et al.*, *Phys. Rev. Lett.* **95**, 247002 (2005)
 - [3] Y. Wang, L. Li, and N.P. Ong, *Phys. Rev. B* **73**, 024510 (2006)
 - [4] R. Bel, K. Behnia, and H. Berger, *Phys. Rev. Lett.* **91**, 066602 (2003)
 - [5] A. Pourret *et al.*, *Nature Physics* **2**, 683 (2006)
 - [6] E.H. Sondheimer, *Proc. Roy. Soc. A* **193**, 484 (1948)
 - [7] V.J. Emery, and S.A. Kivelson, *Nature* **374**, 434 (1995)
 - [8] D.S. Fisher, M.P. A. Fisher, and D. A. Huse, *Phys. Rev. B* **43**, 130 (1991)
 - [9] P.W. Anderson, *Nature Physics* (2006)
 - [10] I. Ussishkin, S. L. Sondhi, and D. A. Huse, *Phys. Rev. Lett.* **89**, 287001 (2002)
 - [11] I. Ussishkin, unpublished notes
 - [12] S. Mukerjee and D. A. Huse, *Phys. Rev. B* **70**, 014506 (2004)
 - [13] N. R. Cooper, B. I. Halperin, and I. M. Ruzin, *Phys. Rev. B* **55**, 2344 (1997)
 - [14] P. C. Hohenberg and B. I. Halperin, *Rev. Mod. Phys.* **49**, 435 (1977)
 - [15] V. Oganesyan, D.A. Huse, and S. L. Sondhi, *Phys. Rev. B* **73**, 094503 (2006)
 - [16] P. C. Martin, E. D. Siggia, and H. A. Rose, *Phys. Rev. A* **8**, 423 (1973)
 - [17] S. Raghu, D. Podolsky, and A. Vishwanath, to be published.
 - [18] K. M. Paget, B. R. Boyce, and T. R. Lemberger, *Phys. Rev. B* **59**, 6545 (1999)
 - [19] P.A. Lee and X.G. Wen, *Phys. Rev. Lett.* **78**, 4111 (1997)
 - [20] C. Honerkamp and P.A. Lee, *Phys. Rev. Lett.* **92**, 177002 (2004)